PHYSICAL REVIEW B VOLUME 14, NUMBER 12 15 DECEMBER 1976

Hot-electron effects in silicon quantized inversion layers

D. K. Ferry
Office of Naval Research, Arlington, Virginia 22217
(Received 2 July 1976)

The mobility variations and carrier velocities are calculated for electrons in (100)-silicon quantum inversion layers at 300 and 77 K. Energy and momentum relaxation by intervalley phonons and acoustic phonons is considered. Scattering by local potential fluctuations and surface roughness is also considered. The calculations performed are based on a drifted Maxwellian distribution function and take into account repopulation of carriers among the various subbands. Formulas are presented for energy and momentum loss by intervalley phonons in both the zero- and first-order coupled cases. The calculations are compared with the data of Fang and Fowler at 300 K and very good agreement is found for the velocity-field curve.

I. INTRODUCTION

When an electric field is applied to the surface of a p-type semiconductor, such as occurs in a metal-oxide-semiconductor structure under bias, an n-type inversion layer is produced at the surface. When the bands are strongly bent, as in strong inversion, the potential well formed by the insulator-semiconductor surface and the electrostatic potential in the semiconductor can be narrow enough that quantum-mechanical effects become important. The motion of the electrons in the direction perpendicular to the surface is constrained to remain within this potential well, and if the thickness is comparable to the electron wavelength, size-effect quantization leads to widely spaced subbands of electron energy levels. The electron energy levels are grouped into the subbands, each of which corresponds to a particular quantized level formation in the direction perpendicular to the surface.[1] In the case of silicon, the transport of electrons within the inversion layer remains dominated by intervalley and acoustic phonons, at least for temperatures greater than or of the order of liquid-nitrogen temperatures, although other scattering mechanisms are also of importance. The role of intervalley scattering by both zero-order coupled and first-order coupled phonons was examined previously, both in bulk silicon[2] and in the inversion layer[3] by the present author (hereafter referred to as I).

In the presence of high electric fields, it is well known that electron transport becomes non-Ohmic.[4] Carriers gain energy from the electric field and must lose this energy to the lattice through collisions. As a rule, the average energy of the electron gas increases with a consequent decrease in the collisional momentum relaxation time. Detailed measurements of the changing electron velocity in the inversion layer as a function of the drain-source field have been presented by Fang and Fowler.[5] To date, an adequate treatment of the drift velocity in these n-type inversion layers in silicon is lacking. Hess and Sah[6] did carry out a theoretical analysis, but they effectively treated only a single phenomenological optical phonon with an adjustable coupling strength. As a consequence, even though they adjust this parameter to obtain a reasonable fit to the experimental data, such an approach does not adequately explain the data. For example, their procedure then yields a theoretical curve which predicts a velocity at 77 K some 2–3 time greater than *bulk* silicon, a somewhat unphysical result. Nakamura[7] also considered hot-electron transport, but treated only an energy balance equation and included an empirical temperature dependence of the mobility. He also primarily treated a single intervalley phonon with an adjustable coupling constant. As discussed in I, the electron transport is considerably more complex than assumed by these authors, and the phonon coupling constants can be taken from their bulk values instead of being treated as adjustable parameters. The purpose of this paper is to treat the high-field transport by including properly the appropriate intervalley phonon interactions and utilize the bulk coupling constants. It is shown that this technique yields very good agreement to experimental data without resorting to adjustable parameters.

In this paper, the momentum and energy relaxation times for hot electrons constrained to a quasi-two-dimensional layer are developed for the situation in which the symmetric part of the distribution function of the electrons in each subband is Maxwellian with a characteristic temperature T_{ei}, where i refers to the subband of interest. The assumption of a characteristic temperature is clearly valid for the case of strong inversion, since interelectronic collisions here will randomize the momentum. In Secs. II and III, the momentum and energy relaxation times, respectively,

are developed for the zero-order and first-order coupled intervalley phonons that are of importance here. In Sec. IV, repopulation of the valleys is discussed and valley-to-valley transition rates for the intervalley phonon processes are developed. Finally, in Sec. V, these results are applied to electrons in an inversion layer on (100) silicon at 300 and 77 K and it is shown that good agreement is obtained with experiment using the coupling constants found in previous work. No adjustable constants in the acoustic or intervalley scattering are used in these calculations. Although local-potential scattering and surface-roughness scattering are included, and their strengths can be adjusted to fit the Ohmic mobility, it must be emphasized that the high-field, hot-electron behavior is governed by the intervalley scattering interactions. As a result, the high-field behavior is essentially independent of the local-potential and surface-roughness scattering.

II. MOMENTUM RELAXATION

Treatment of hot-electron problems via the assumption of a drifted Maxwellian distribution function generally revolves around the use of a pair of balance equations which require equilibration of both the average momentum and the average energy of the electron gas.[4,8,9] We will treat the first of these in this section and defer discussion of the other until Sec. III. The momentum balance equation requires that the rate at which momentum is supplied to the electrons by the electric field be offset by loss of momentum to the lattice, or

$$eE = \left\langle \frac{dp}{dt} \right\rangle = m_c v_d \left\langle \frac{1}{\tau} \right\rangle , \tag{1}$$

where the last form follows for a drifted Maxwellian

$$f(\vec{k}) = C \exp[-\hbar^2(\vec{k} - \vec{k}_d)^2/2m_c k_B T_e], \tag{2}$$

where $\hbar k_d = m_c v_d$ is the average drift momentum of the electron gas, C is a constant for normalization purposes, and T_e is the electron temperature. From (2), it follows that

$$f_0(E) = Ce^{-E/k_B T_e} \tag{3}$$

and

$$f_1(E) = v(m_c v_d/2k_B T_e) f_0(E). \tag{4}$$

From (1) and (4), the average momentum relaxation rate is shown to be just

$$\left\langle \frac{dp}{dt} \right\rangle = \left\langle \frac{mv}{\tau} \right\rangle = m_c v_d \left\langle \frac{1}{\tau} \right\rangle , \tag{5}$$

where

$$\left\langle \frac{1}{\tau} \right\rangle + \left[\int \left(\frac{1}{\tau} \right) y e^{-y}\, dy \right] \left(\int e^{-y}\, dy \right)^{-1} = \int \left(\frac{1}{\tau} \right) y e^{-y}\, dy , \tag{6}$$

where $y = E/k_B T_e$. The explicit form of (6) follows from the fact that in quasi-two-dimensional systems, the density of states is independent of the electron energy.[1] Thus, (6) gives the phenomenological momentum relaxation time or, more properly, the momentum relaxation rate.

The scattering rate for interactions via the zero-order coupled intervalley phonons was shown in I to be, for electrons in subband i in valley a,

$$\frac{1}{\tau} = \frac{D^2}{\rho_m \hbar^2 \omega_0} \sum_{j,b} I_{ij} \frac{(m_{1b} m_{2b})^{1/2}}{2w_j} \{ N u_0(E - E_j + \hbar\omega_0)[1 - f_0(E + \hbar\omega_0)] + (N+1) u_0(E - E_j - \hbar\omega_0)[1 - f_0(E - \hbar\omega_0)] \}, \tag{7}$$

where D is the coupling deformation potential, ρ_m is the mass density, I_{ij} is the square of the wave function overlap integral between the electrons in the initial subband i and the final subband j in valley b, w_j is the level width of the jth subband for the bth set of valleys, m_{1b} and m_{2b} are the two masses in the directions parallel to the surface, N is the Bose-Einstein occupation factor for the phonon of circular frequency ω_0, and E_j is the energy level of the jth subband. The sum runs over all subbands and levels, that is over all final states coupled by the particular phonon. The first term in the curly brackets is for phonon absorption by the electron and the second term is for phonon emission by the electrons. The functions $u_0(x)$ are step functions and are equal to unity for $x \geq 0$ and zero otherwise. The terms in the square brackets allow for degeneracy of the distribution function. These latter factors will not be carried further since these effects are of limited applicability for hot electrons,[6] due to the high effective temperature of the distribution. Inserting (7) into (6) and evaluating the integrals gives, for scattering from subband i in valley a to subband j in valley b,

$$\left\langle \frac{1}{\tau} \right\rangle_0 = \frac{D^2 (m_{1b} m_{2b})^{1/2} \beta_b}{\rho_m \hbar^2 w_j \omega_0} \left[\left(\frac{e^{x_0 - x_{ei}} + 1}{e^{x_0} - 1} \right)(1 + \Delta_{ij}) + \left(\frac{x_{ei} e^{x_0 - x_{ei}}}{e^{x_0} - 1} \right) \right] e^{-\Delta_{ij}}, \tag{8}$$

where $x_0 = \hbar\omega_0/k_B T_0$, T_0 is the lattice temperature, $x_{ei} = \hbar\omega_0/k_B T_{ei}$, β_b is the number of equivalent valleys

of the final subband to which the electron can scatter, and $\Delta_{ij}=(E_j-E_i)/k_BT_{ei}$ ($E_j \geq E_i$ only). T_{ei} is the effective temperature in subband i. In the case that $T_{ei}=T_0$ and $E_j=E_i$, (8) reduces to Eq. (14) of I.

For the first-order coupled interaction, the phonon scattering rate was also found in I. For electrons in subband i in valley a, this is just

$$\frac{1}{\tau'}=\frac{D_1^2}{\rho_m\hbar^4\omega_0}\sum_{j,b}I_{ij}\frac{m_{1b}m_{2b}}{w_j}[N(2E+\hbar\omega_0)u_0(E-E_j+\hbar\omega_0)+(N+1)(2E-\hbar\omega_0)u_0(E-E_j+\hbar\omega_0)], \tag{9}$$

where the symbols have their previous meanings, and D_1 is the value of the first-order coupling constant. Using (9) in (6), the momentum relaxation rate due to first-order coupled phonons is found to be, for scattering from subband i in valley a to subband j in valley b,

$$\left\langle\frac{1}{\tau}\right\rangle_1=\frac{2D_1^2m_{1b}m_{2b}\beta_b}{\rho_m\hbar^3w_j}\left\{\left(\frac{e^{x_0-x_{ei}}+1}{e^{x_0}-1}\right)\left[\frac{2}{x_{ei}}\Delta_{ij}^2+\left(\frac{4}{x_{ei}}+1\right)(1+\Delta_{ij})\right]+\left(\frac{e^{x_0-x_{ei}}}{e^{x_0}-1}\right)(2+x_{ei}+2\Delta_{ij})\right\}e^{-\Delta_{ij}}. \tag{10}$$

In addition to the intervalley scattering, interactions due to acoustic phonons and local-potential scattering are considered. Kawaji[10–12] and Sah *et al.*[13] have calculated the acoustic-phonon mobility. The momentum relaxation rate for this process is given by

$$1/\tau_{ac}=[(m_{1b}m_{2b})^{1/2}\Xi_1^2k_BT_0/\hbar^2\rho_mw_jv_s^2]\lambda, \tag{11}$$

where Ξ_1 is the acoustic deformation potential and v_s is the sound velocity. The functional parameter λ depends on the overlap integral of the wave functions and differs for bulk phonon or surfon scattering.[10–12] The other parameters have their usual meaning. Equation (11) contains no dependence on the electron temperature or electron kinetic energy, so that the momentum relaxation rate depends only upon the lattice temperature.

For scattering by local potentials, arising from ionized impurities or trapped interface charge, the phenomenological form developed by Sah *et al.*[12] is used. In this form, the momentum relaxation rate is given by

$$\langle 1/\tau\rangle_I=Ge^4\pi^2N_I/2\epsilon^2\hbar k_BT_{ei}, \tag{12}$$

where G is a global multiplicative factor to take account of screening, spatial charge distribution, and position correlation effects as well as any other factors not understood. For surface roughness scattering, the relaxation rate can be taken from Stern,[1] and is given by

$$\frac{1}{\tau_{sr}}=\frac{L^2\delta^2\hbar(m_{1b}m_{2b})^{1/2}(3)^6}{16m_{3b}^2w_j^6}e^{-k^2L^2/2}\times[I_0(k^2L^2/2)-I_1(k^2L^2/2)], \tag{13}$$

where δ is the mean-square height of the deviation of the surface from flatness, and L is the lateral scale length of the fluctuations, and I_0 and I_1 are modified Bessel functions of the first kind. When $kL<1$, the scattering rate of (13) is independent of carrier energy, and even when this inequality is not satisfied, the right-hand side of (13) is a very slowly varying function. The factor G and the product $L\delta$ are the only adjustable parameters in this work. Although the high-field treatment of the transport properties is essentially independent of their values, these values must be chosen judiciously in order to obtain a good fit to the low-field Ohmic mobility.

III. ENERGY RELAXATION

The second balance equation requires that the average rate of energy which the electron gas gains from the field be balanced by a loss of energy to the lattice. This requires that

$$ev_dE=-\left\langle\frac{dE}{dt}\right\rangle. \tag{14}$$

It can be seen that the pair of equations (1) and (14) contain only two unknown parameters, the drift velocity v_d and the effective temperature T_{ei} in a particular valley. We will discuss below the way in which the knowledge of the individual valleys can be combined to give the resulting parameters for the electron gas as a whole.

For optical and intervalley phonons, the right-hand side of (14) is given for a particular phonon by

$$-\frac{dE}{dt}=\hbar\omega_0\left[\left(\frac{1}{\tau}\right)_e-\left(\frac{1}{\tau}\right)_a\right], \tag{15}$$

where the first term in brackets is the scattering rate for emission of phonons and the second term is the scattering rate for the absorption of phonons. The average is carried out using (2), and to lowest order

$$\left\langle\frac{dE}{dt}\right\rangle=\int\left(\frac{dE}{dt}\right)e^{-y}\,dy. \tag{16}$$

By changing the appropriate signs on the terms in (7) it can be used in (12) to give the average energy loss associated with scattering by zero-order coupled phonons from subband i in valley a to sub-

band j in valley b, as

$$-\left\langle\frac{dE}{dt}\right\rangle=\frac{D^2(m_{1b}m_{2b})^{1/2}\beta_b}{\rho_m\hbar w_j}\left(\frac{e^{x_0-x_{ei}}-1}{e^{x_0}-1}\right)e^{-\Delta_{ij}}. \quad (17)$$

Similarly, from (9) the average energy loss associated with scattering by first-order coupled phonons from subband i in valley a to subband i in valley b is found to be

$$-\left\langle\frac{dE}{dt}\right\rangle=\frac{2D_1^2m_{1b}m_{2b}\beta_bk_BT_{ei}}{\rho_m\hbar^3w_j}\left(\frac{e^{x_0-x_{ei}}-1}{e^{x_0}-1}\right)\times[2(1+\Delta_{ij})+x_{ei}]e^{-\Delta_{ij}}. \quad (18)$$

The acoustic-phonon scattering and local-potential scattering are essentially elastic and do not contribute to any appreciable energy relaxation. Their effects in energy relaxation will be ignored in this work.

IV. REPOPULATION

In semiconductors with multivalley band structures, hot-electron conditions can alter the relative populations of the various valleys due to different temperatures in the various valleys. This is also true in the inversion layers, where the relative populations of the various subbands in each valley can also be expected to be modified. The equilibrium equation for a particular subband can be written, in analogy with the multivalley case,[4,14]

$$\frac{dn_i}{dt}=-\sum_j\left(\frac{\partial n_i}{\partial t}\right)_{c,i\to j}+\sum_j\left(\frac{\partial n_i}{\partial t}\right)_{c,j\to i}, \quad (19)$$

where the sum runs over all subbands $j\neq i$. The subscript c on the right-hand-side terms refers to collision-induced transitions. In Sec. V, three subbands will be used in the calculations: n_1,n_2,n_3 (for levels of energy E_0,E_1,E_0', respectively, in the notation of I and Ref. 1). The meaning and labeling of these subbands is explained below. To coordinate with this, let us now adopt a three-level scheme for illustration. Then we can write

$$\frac{dn_1}{dt}=-\int(\Gamma_{12}+\Gamma_{13})n_1(E)C_1e^{-E/k_BT_{e1}}dE+\int\Gamma_{21}n_2(E')C_2e^{-E'/k_BT_{e2}}dE'+\int\Gamma_{31}n_3(E'')C_3e^{-E''/k_BT_{e3}}dE'', \quad (20)$$

where the integrals run over all the states in each subband, and Γ_{ij} is the *total* scattering rate from level i to level j. Now, (20) can be rewritten

$$\frac{dn_1}{dt}=-(\alpha_{12}+\alpha_{13})n_1+\alpha_{21}n_2+\alpha_{31}n_3, \quad (21)$$

where n_i is the total number of electrons in level i [as opposed to the density of states $n_i(E)$ of level i]. The parameter α_{ij} is just

$$\alpha_{ij}=\left(\int\Gamma_{ij}n_i(E)C_ie^{-E/k_BT_{ei}}dE\right)\left(\int n_i(E)C_ie^{-E/k_BT_{ei}}dE\right)^{-1}=\int\Gamma_{ij}e^{-y}dy\ , \quad (22)$$

where once again $y=E/k_BT_{ei}$. Although the contribution to Γ_{ij} is just the scattering rate $1/\tau$, the average in (22) is not the same as that leading to the momentum relaxation rate and thus α_{ij} is not just $\langle 1/\tau\rangle$. Rather, the average is that appropriate to the energy relaxation time, although the signs on the various contributions are different. Thus, we can use (7) and (9) in (22) to give the contributions to α_{ij} due to zero-order coupled phonons and first-order coupled phonons, respectively. These are just, for scattering from level i in subband a to level j in subband b,

$$\alpha_{ij,0}=\frac{D^2(m_{1b}m_{2b})^{1/2}\beta_b}{\rho_m\hbar^2w_j\omega_0}\left(\frac{e^{x_0-x_{ei}}+1}{e^{x_0}-1}\right)e^{-\Delta_{ij}} \quad (23)$$

and

$$\alpha_{ij,1}=\frac{2D_1^2m_{1b}m_{2b}\beta_bk_BT_{ei}}{\rho_m\hbar^4w_j\omega_0}\left(\frac{e^{x_0-x_{ei}}+1}{e^{x_0}-1}\right)(2+x_{ei})e^{-\Delta_{ij}}\ . \quad (24)$$

Equations similar to (21) can also be written for either levels n_2 or n_3, but not both as the set of three yield only two independent equations. The third equation is just the conservation of the total density

$$n_s=n_1+n_2+n_3\ . \quad (25)$$

These equations can then be solved in a straightforward manner to yield the fractional occupations n_1/n_s, n_2/n_s, and n_3/n_s in terms of the various coupling constants α_{ij}.

It should be noted at this point that the rate at which scattering occurs both within a particular level and out of that level depends only upon the characteristic electron temperature T_{ei} of that level. Thus, a set of two balance equations can be solved independently for the velocity-field characteristics of each level and the three levels joint total velocity-field characteristics found through determining the total current. Since $J=n_sev_d$, then

the partial occupations of the three levels found above can be used to find the effective velocity as

$$v_d = (n_1/n_s)v_{d1} + (n_2/n_s)v_{d2} + (n_3/n_s)v_{d3} . \quad (26)$$

V. ELECTRON INVERSION LAYERS IN SILICON

In a quantized electron inversion layer at the surface of (100)-oriented silicon, the six equivalent minima of the bulk silicon conduction band split into two sets of subbands. One set consists of the subbands arising from the two valleys which show the longitudinal mass in the direction perpendicular to the surface. This set has energy levels E_0, E_1, E_2, ... in the notation of Stern and Howard.[15] The lowest subband at the surface E_0 belongs to this set. The other set of subbands arises from the four equivalent valleys which show a transverse mass in the direction normal to the surface. This set has energy levels designated as E_0', E_1', E_2', ... Generally, these levels line up such that E_0' is almost degenerate with E_1. Except at very low temperatures, it is unreasonable to assume that all of the electrons are in the lowest subband. However, it is not a bad approximation to assume that most of the electrons occupy the three lowest levels E_0, E_1, and E_0', and this was done in I. This approximation will also be taken in the present work. As mentioned above, the valleys are uncoupled in the two balance equations and these can be solved for each valley separately to determine its parameters. Then the fractional occupations of the valleys are found from the transition rate equations of the previous section and the total effective mobility or velocity is found.

Scattering between the two equivalent valleys in the E_0 and E_1 subbands involves g-type phonons.[3,16] These phonons couple the [001] valley with its partner along the [00$\bar{1}$] direction. In the present calculation, the scattering between these two minima will be treated by using a high-energy phonon of 750-K equivalent activation temperature ($T_a = \hbar\omega_0/k_B$) and a low-energy phonon of 134-K equivalent activation temperature. The former is chosen as it is the value of the LO phonon that is allowed in the g process. It is treated via a zero-order interaction. The 134-K phonon is found to be the strongest low-energy g phonon in magnetophonon resonance studies in silicon.[17] This phonon is forbidden in zero-order[18,19] and will be treated by a first-order interaction.

Scattering between the two subbands E_0, E_1, and the four E_0' subband valleys involves f-type phonons.[3,16]. For this scattering, which is primarily responsible for repopulation among the subbands, f phonons of 630- and 230-K equivalent activation temperatures are utilized. The former is zero-order coupled while the latter is the value of the zone-edge TA phonon which is forbidden to zero order. This is treated via the first-order interaction.

Scattering between the valleys of the E_0' subband involves both the g- and f-type phonons. As in I, it is a viable procedure to use just two effective phonons of 630 and 190 K for these phonons, as is also done in treating bulk silicon. The former is zero-order coupled while the latter is first-order coupled since all phonons which could contribute to this low-temperature interaction are forbidden. In this work, as in I and in bulk silicon,[2] all of the high-energy phonons are assumed to be coupled with a value of $D = 9 \times 10^8$ eV/cm and all of the first-order coupled phonons are assumed to be coupled with $D_1 = 5.6$ eV. A value of $\Xi_1 = 12$ eV, appropriate to the surface,[11] is taken for the deformation potential of acoustic scattering. The values of the unknown constants $G(GN_I = 2.5 \times 10^{10}$ cm^{-2}) and $L\delta(0.5$ Å^2) were taken so that the total calculated mobility for $n_s = 10^{12}$/cm^2 at 300 K agreed with the experimental data of Fang and Fowler,[20] used in I. This value was then considered constant throughout the rest of the calculations.

The values for the various masses are their normal values and are tabulated in Stern[1] and Howard.[15] The level thicknesses w_j are taken from the self-consistent calculations reported in the same references and from estimates made using a triangular-well approximation. Their variation as well as the variation of the energy levels with temperature of the lattice is explicitly taken into account.

The calculated low-field Ohmic mobilities for electrons is 600 cm^2/V sec at 300 K and 2500 cm^2/V sec at 77 K for an inversion density of $n_s = 10^{12}$/cm^2. For $n_s = 10^{13}$/cm^2, a mobility at 300 K of 390 cm^2/V sec is calculated. In Fig. 1, the velocity is shown as a function of electric field at 300 K for $n_s = 10^{12}$/cm^2 and $n_s = 10^{13}$/cm^2 for (100) silicon. The mobility increases above the Ohmic value for fields in the range 10^2–10^3 V/cm, due primarily to the falloff of local potential scattering as T_e increases. For fields above 10^3 V/cm, the lower subbands are becoming very hot and carrier transfer into the E_0' valley begins. This upper valley remains relatively cool for fields below 20 kV/cm. For fields above this, however, heating of this upper set of valleys begins to become significant and the repopulation will eventually redistribute the carriers equally among all valleys at very high fields. The carrier transfer from the E_0 and E_1 valleys to the E_0' valley can be seen in the velocity-field curves as an inflection point. It is most prevalent in Fig. 1 in the curve for $n_s = 10^{13}$/cm^2 at a field in the vicinity of 10^4 V/cm. The relative

populations of the E_0 and E_0' subbands are shown in Fig. 2 for $n_s = 10^{12}/cm^2$ and in Fig. 3 for $n_s = 10^{13}/cm^2$. The experimental data of Fang and Fowler[5] for $n_s = 6.6 \times 10^{12}/cm^2$ is also shown in Fig. 1. It can be seen that the agreement is very good with this data. It can also be seen in Fig. 1, that when the upper valleys begin to become hot, the direction of the field is important, since all four valleys are equivalent only for a field along the ⟨110⟩ direction. For other field directions, redistribution among these valleys becomes important.

The velocity-field curve calculated for $n_s = 10^{12}/cm^2$ at 77 K is shown in Fig. 4. Hot-electron effects and repopulation of the various valleys set in at much lower electric fields at this temperature. Significant repopulation results in an inflection point in the velocity-field curve in the region around 200 V/cm. The relative populations of the E_0 and E_0' subbands are shown in Fig. 5. Repopulation occurs over a relatively narrow range of electric field and is essentially complete by a field of 300 V/cm. Even though the large population shift occurs from the light mass E_0 valley to the heavy mass E_0' valley, the velocity increases

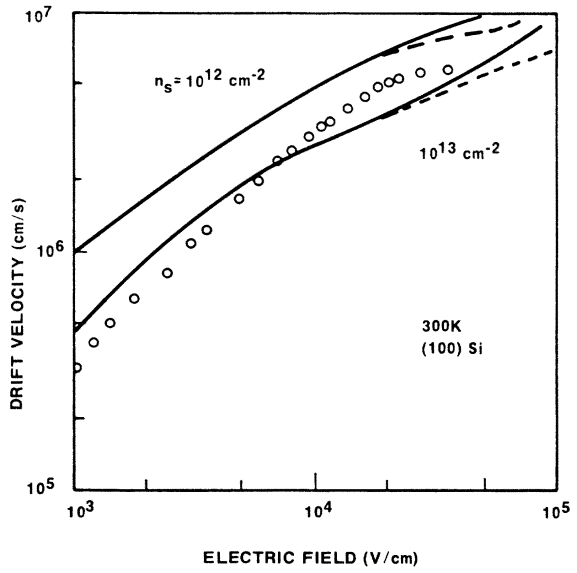

FIG. 1. Velocity-field curves calculated for $n_s = 10^{12}/cm^2$ and $n_s = 10^{13}/cm^2$, on (100) silicon, are shown. The data of Fang and Fowler (Ref. 5) for $n_s = 6.6 \times 10^{12}/cm^2$ are indicated by the open circles. The solid curves are for the drain-source electric field parallel to the [011] direction, so that the four valleys of the E_0' subband make the same angle with the field and are thus equivalent. The dashed curves are for the drain-source electric field parallel to the [010] direction, for which repopulation occurs among the four valleys of the E_0' subband as it becomes hot.

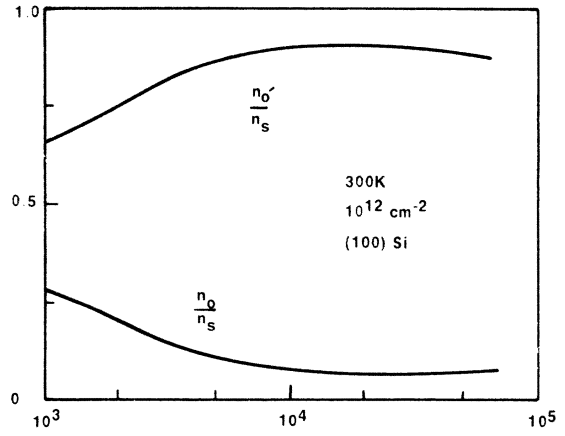

FIG. 2. Relative populations of the E_0 and E_0' subbands are shown as a function of the electric field for $n_s = 10^{12}/cm^2$ at 300 K.

monotonically with the electric field, as can be seen in Fig. 4. No negative differential conductivity exists in this system, at least for the values utilized in the present calculation. Hess and Sah[6] show such an effect occurring at 77 K, although at much higher fields, so that it can only be speculated that it arises in their calculations from repopulation. It would indeed be surprising if such an effect did occur since the ratio of the densities of states for these two sets of valleys is so low, being essentially only about 4. However, negative differential conductivity due to equivalent valley repopulation is known in bulk silicon, in the case that the electric field makes different angles with the individual valleys, although this effect occurs at lower temperatures.[21] The onset of this insta-

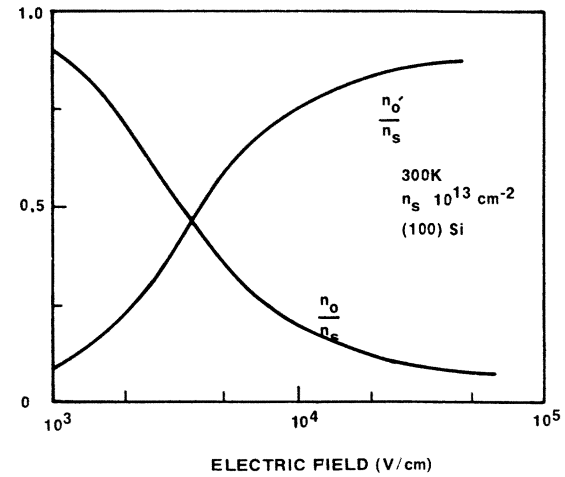

FIG. 3. Relative populations of the E_0 and E_0' subbands are shown as a function of the electric field for $n_s = 10^{13}/cm^2$ at 300 K.

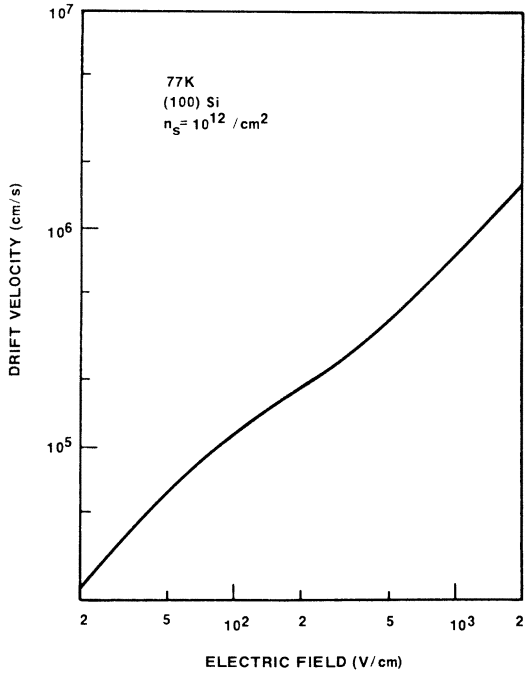

FIG. 4. Drift velocity of electrons calculated for $n_s = 10^{12}/\text{cm}^2$ is shown at 77 K as a function of the drain-source electric field. For these values of the field, the upper E_0' subband remains relatively cool so that there is effectively no difference among the various directions lying in the surface.

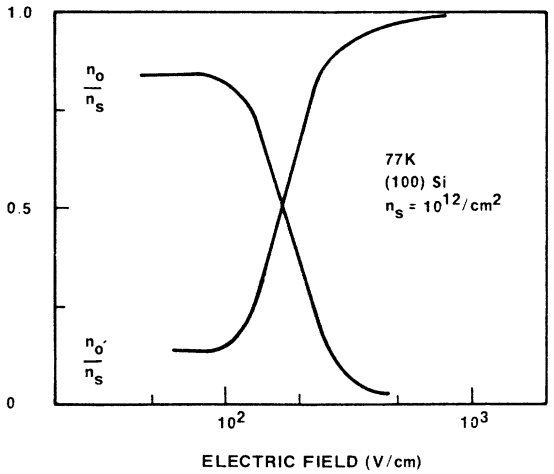

FIG. 5. Relative populations of the E_0 and E_0' subbands are shown as a function of the electric field for $n_s = 10^{12}/\text{cm}^2$ and 77 K.

bility actually occurs at fields very near to those for which repopulation occurs in the present calculations, so that there is good confidence in the current calculations and one can not rule out the possibility that negative differential conductivity could occur in the inversion layer for some values of surface carrier density.

VI. CONCLUSIONS

The inclusion of intervalley scattering in treating the transport of electrons in inversion layers in silicon yields very good agreement with those experimental data that are available. The results found here include both zero-order and first-order coupled intervalley phonons and takes account of the repopulation among the three lowest subbands. Repopulation of the various subbands results in transfer of most of the carriers out of the E_0 and E_1 subbands into the heavy mass E_0' subband. However, at very high fields, above 10^5 V/cm at 300 K, this process is reversed as the heavy-mass valleys become hot. At these very high fields, the carriers are sufficiently hot that the inversion layer appears bulklike. with the carriers equally distributed among the various valleys. In fact, the saturated velocity approaches that of bulk material, approximately 10^7 cm/sec. The role of other subbands is not expected to change the results much. Although the higher subbands show larger mobilities due to an increase in w_j, they get hot at lower applied electric fields, so that the net effect does not modify the high-field behavior to any great extent.

At 77 K, the repopulation occurs at much lower fields, in fact at fields close to where it occurs in bulk material[21] for E along a $\langle 100 \rangle$ direction. Although repopulation occurs, the velocity-field curve remains monotonic in character and there is no evidence of any negative differential conductivity. The ratio of densities of states for the valleys on (100) silicon is only about 4, a value that should be too low at these temperatures to generate any negative differential conductivity. For example, in GaAs this effect occurs in the bulk material when carriers transfer from the central valley of the conduction band to the subsidiary valleys lying along the [100] directions. However, the ratio of densities-of-states in that case is about 70, more than an order of magnitude larger than in the present case. In silicon, the effect is known to occur at much lower temperatures for repopulation among the [100] valleys when the electric field does not make the same angle with all of the valleys. Again in the case at 77 K, as at 300 K, for still higher fields than those shown, the velocity saturates near the bulk value of 10^7 cm/sec.[22]

In conclusion, it has been shown that hot-electron transport in inversion layers at a silicon surface is dominated by intervalley scattering. When proper treatment of all necessary phonons is in-

cluded, results agree well with experimental data. This good agreement is obtained by utilizing values for the deformation potentials that agree with bulk values. Although agreement at a single temperature can also be obtained by using a single phonon and adjusting the coupling constant,[6,7] the incorporation of all the important phonons avoids this *ad hoc* procedure.

[1]For a general review, see F. Stern, Crit. Rev. Solid State Sci. 4, 499 (1974).
[2]D. K. Ferry, Phys. Rev. B 14, 1605 (1976).
[3]D. K. Ferry, Surf. Sci. 57, 218 (1976).
[4]See, e.g., E. Conwell, *High Field Transport in Semiconductors* (Academic, New York, 1967).
[5]F. F. Fang and A. B. Fowler, Phys. Rev. 41, 1825 (1970).
[6]K. Hess and C. T. Sah, J. Appl. Phys. 45, 1254 (1974); Phys. Rev. B 10, 3375 (1974).
[7]K. Nakamura, *International Conference on Electronic Properties of Quasi-Two-Dimensional Systems, Providence, Rhode Island, Aug. 25–28, 1975* (North-Holland, Amsterdam, 1976), p. 48.
[8]R. Stratton, Proc. R. Soc. Lond. A 242, 355 (1957); 246, 406 (1958).
[9]D. K. Ferry, Phys. Rev. B 12, 2361 (1975).
[10]S. Kawaji, J. Phys. Soc. Jpn. 27, 608 (1967).
[11]H. Ezawa, T. Kuroda, and K. Nakamura, Surf. Sci. 24, 659 (1971).
[12]H. Ezawa, S. Kawaji, and K. Nakamura, Surf. Sci. 27, 218 (1971); J. Appl. Phys. 13, 126 (1974).
[13]C. T. Sah, T. H. Ning, and L. L. Tschopp, Surf. Sci. 32, 561 (1972).
[14]H. Heinrich and M. Kriechbaum, J. Phys. Chem. Solids 31, 927 (1970).
[15]F. Stern and W. E. Howard, Phys. Rev. 163, 816 (1967).
[16]The notation is that of D. Long [Phys. Rev. 120, 2024 (1960)] who considered the effect of intervalley phonons on transport in bulk silicon.
[17]J. C. Portal, L. Eaves, S. Askenazy, and R. A. Stradling, in *Proceedings of the Twelfth International Conference on the Physics of Semiconductors, Stuttgart*, edited by M.H. Pilkuhn (Teubner, Stuttgart, 1974), p. 259.
[18]H. W. Streitwolf, Phys. Status Solidi 37, K47 (1970).
[19]M. Lax and J. L. Birman, Phys. Status Solid B 49, K153 (1970).
[20]F. Fang and A. B.Fowler, Phys. Rev. 169, 619 (1968).
[21]N. O. Gram, Phys. Lett. A 38, 235 (1972).
[22]J. G. Nash and J. W. Holm-Kennedy, Appl. Phys. Lett. 27, 38 (1975).